# Collective excitations in a single-layer carbon nanotube

M. F. Lin, D. S. Chuu, C. S. Huang, and Y. K. Lin
*Electrophysics Department, National Chiao Tung University, Hsinchu 30050, Taiwan, Republic of China*

K. W. -K. Shung
*Physics Department, National Tsing Hua University, Hsinchu 30043, Taiwan, Republic of China*
(Received 19 October 1995; revised manuscript received 1 February 1996)

The inter-$\pi$-band response function of a single-layer carbon nanotube is calculated within the random-phase approximation. Such a cylindrical system exhibits rich inter-$\pi$-band excitations. The decoupled $\pi$ plasmons of different angular momenta ($L$'s) strongly depend on the transferred momenta ($q$'s). Furthermore, they exhibit a dimensionality crossover as the nanotube radius is increased. For small $q$'s and $L$'s, the $\pi$ plasmon frequency is ~6–8 eV, which is insensitive to the nanotube geometry such as the radius and chiral angle. Comparison with recent experiments is discussed. [S0163-1829(96)02823-8]

A system purely made up of carbons, namely, carbon nanotubes, was recently discovered by Iijima.[1] A carbon nanotube consists either of a single tubule or of several coaxial tubules with a radius 10–150 Å. Furthermore, carbon atoms are arranged on each cylindrical tubule in a helical fashion. Such a cylindrical nanotube represents an interesting class of quasi-one-dimensional (1D) system, and has stirred many studies on the electronic structure[2–6] and excitations.[7–17] The band property is predicted to be either metallic or semiconducting, which depends on the radius and chiral angle.[2–6] Studies[7–17] of electronic excitations are very important in understanding the electron interactions in carbon nanotubes as well as the characteristics of their band structure. Electronic excitations due to optical processes have been studied theoretically for a 3D nanotube bundle by evaluating the transverse dielectric function.[7] In this work the inter-$\pi$-band excitations of a single-layer carbon nanotube are further investigated by evaluating the longitudinal dielectric function within the random-phase approximation (RPA).[18] We mainly study the $\pi$-band plasmons with frequencies larger than 5 eV, and their dependence on momentum ($q$), angular momentum ($L$), and nanotube geometry.

The $\pi$ and $\sigma$ bands in a carbon-based $sp^2$ system are formed, respectively, by $2p_z$ and $(2s,2p_x,2p_y)$ orbitals. There have been some experiments[8–11] on the electron-energy-loss spectrum (EELS) of a multilayer carbon nanotube. These measurements show that the $\pi$ plasmon frequency is ~5–7 eV,[8–11] the $\pi+\sigma$ plasmon frequency ~22–27 eV,[8–10] and the surface plasmon frequency ~15 eV.[10] The plasmon frequencies of carbon nanotubes are close to those [~7 and 25 eV (Ref. 19)] of graphite. On the theoretical side, the elementary excitations in a cylindrical nanotube are studied within the 1D electron-gas model, either by neglecting[12–16] or including[17] (within the Hartree-Fock approximation) the electron interactions. These studies, respectively, focus on the conduction[12–14] and valence[15,17] electrons of the $\pi$ band, and the $\sigma$ electrons.[16] Due to cylindrical symmetry, $q$ in the axial direction and $L$ about the nanotube axis are conserved in the electron interactions. Hence there are many decoupled plasmons, each with a specific $L$. Moreover, the plasmon frequencies strongly depend on $q$ (Refs. 12–17) and the applied magnetic flux.[12,14,17] The $\pi$ plasmon frequency[17] is predicted to be ~8 or 22–25 eV, and the $\sigma$ plasmon[15] to exhibit a dimensionality crossover when the number of sheets is increased. It should be noted that the existence of the $\pi$ plasmon above 20 eV (Ref. 17) has been questioned. The real band structure,[2–6] however, is not taken into account in these theoretical studies. Electronic excitations directly reflect characteristics of band structure,[7] and, therefore, should be included in the study.

We use the tight-binding model[4,20] to calculate the $\pi$ band, and the RPA to evaluate the dielectric function $[\epsilon(q,L,w)]$. The band-structure effects are strong, and appreciably affect the characteristics of $\epsilon(q,L,w)$, which is very different from that of an electron gas.[12–17] In fact, our study shows that the $\pi$ plasmon, which is the most prominent peak in EELS, mainly reflects the characteristics of the $\pi$ band. Also found is that the $\pi$ plasmon frequencies for different $L$'s steadily increase as $q$ increases. The $\pi$ plasmon frequency is ~6–8 eV at small $q$'s and $L$'s, which is insensitive to the nanotube geometry (e.g., the radii and the chiral angles). This finding could essentially explain the ~5–7-eV plasmon observed in EELS.[8–11]

As has been discussed,[21] a single-layer carbon nanotube is a rolled-up graphite sheet, the structure of which is thus fully specified by a 2D lattice vector $\mathbf{R}_x = m\mathbf{a}_1 + n\mathbf{a}_2$, where $\mathbf{a}_1$ and $\mathbf{a}_2$ are primitive lattice vectors of a graphite sheet. The parameters $(m,n)$, therefore, uniquely define a single-layer carbon nanotube. The chiral angle and the radius of a $(m,n)$ nanotube are, respectively, $\theta = \tan^{-1}[-\sqrt{3}n/(2m+n)]$ and $r = |\mathbf{R}_x|/2\pi = [b\sqrt{3(m^2+mn+n^2)}/2\pi]$. Here $b = 1.42$ Å is the C-C bond length. The $\pi$ band is calculated with the nearest-neighbor tight-binding Hamiltonian like the one employed for a graphite sheet,[20] but here with the properly periodical boundary condition along the transverse direction. The energy dispersions of the $(m,n)$ nanotube, obtained by diagonalizing the Hamiltonian, are[7,21]

 

$$E^{c,v}(k_x,k_y)=\pm\gamma_0\left\{1+4\cos\left(\frac{3b(k_y\cos\theta+k_x\sin\theta)}{2}\right)\times\cos[\sqrt{3}b(k_y\sin\theta-k_x\cos\theta)/2]+4\cos^2\left(\frac{\sqrt{3}b(k_y\sin\theta-k_x\cos\theta)}{2}\right)\right\}^{1/2},\tag{1a}$$

and the wave functions are

$$\Psi^{c,v}(k_x,k_y)=\frac{1}{\sqrt{2}}\left\{U_1(k_x,k_y)\mp\frac{H_{12}^*(k_x,k_y)}{|H_{12}(k_x,k_y)|}U_2(k_x,k_y)\right\}.\tag{1b}$$

The superscript $c$ ($v$) represents the conduction (valence) band. The nearest-neighbor Hamiltonian matrix element is $H_{12}=-\gamma_0\Sigma_{i=1}^{3}e^{-i\mathbf{k}\cdot\mathbf{r}_i}$, where the resonance integral $\gamma_0=3.033$ eV.[4] The axial wave vector $k_y$ is confined within the first Brillouin zone. The transverse wave vector is $k_x=J/r$, where $J=1,2,\ldots,N_u/2$; $N_u$ is the atom number in a primitive unit cell (details in Ref. 21). $J$ is the angular momentum of electrons, and serves as the subband index. The occupied valence bands are symmetric[4,6,2] to the unoccupied conduction bands about the Fermi level $E_F=0$, as obtained from Eq. (1a). Calling all bands below $E_F$ valence bands needs some clarification in the metallic case, e.g., in armchair nanotubes ($\theta=\pm30°$). Metallic nanotubes, upon introducing a magnetic field through the tube, develop a gap at $E_F$.[6] It is thus convenient to treat them as ''gapless'' semiconductors, since the result can then be easily modified to include a magnetic field. With this terminology, the inter-$\pi$-band excitations from the valence to the conduction bands would be the only excitation channel at $T=0$—even for the metallic nanotubes.

Excitations of the system have a well-defined momentum ($q$) and angular momentum ($L$) transfer, and so does the dielectric function. To within the RPA,[18] the dielectric function, which includes all inter-$\pi$-band excitations, is evaluated at $T=0$:

$$\epsilon'(q,L,w+i\Gamma)=\epsilon_0+2\sum_J\times\int_{1\text{stBZ}}\frac{dk_y}{(2\pi)^2}\frac{2w_{vc}(J,k_y;q,L)}{(w_{vc}(J,k_y;q,L))^2-(w+i\Gamma)^2}\times V(q,L)|\langle J+L,k_y+q;c|e^{iqy}e^{iL\phi'}|J,k_y;v\rangle|^2,\tag{2a}$$

where[22]

$$|\langle J+L,k_y+q;c|e^{iqy}e^{iL\phi'}|J,k_y;v\rangle|^2=\tfrac{1}{4}\{1+[q^2+(L/r)^2]/36\}^{-6}\times\left|1-\frac{H_{12}(J+L,k_y+q)H_{12}^*(J,k_y)}{|H_{12}(J+L,k_y+q)H_{12}^*(J,k_y)|}\right|^2.\tag{2b}$$

$w_{vc}(J,k_y;q,L)=E^c(J+L,k_y+q)-E^v(J,k_y)$ is the inter-band excitation energy, $\epsilon_0=2.4$ is the background dielectric constant,[19] $V(q,L)=4\pi e^2I_L(qr)K^L(qr)$ is the Coulomb interaction of an electron gas,[12] and $\Gamma$ is a phenomenological level broadening parameter. $I_L$ ($K_L$) is the first (second) kind of modified Bessel function of the order $L$. The electron interaction is given by the second term in the integrand of Eq. (2a). It includes two parts: $V(q,L)$, which describes the Coulomb interaction for an electron gas, and the inter-$\pi$-band matrix element, which is given by Eq. (2b). The latter is similar in form to that of a graphite sheet.[22] The band-structure effects due to the latter are found to be very important. They modify the Coulomb interaction[12] and, consequently, produce noticeable effects on the physical properties of carbon nanotubes, e.g., EELS and screening properties.[23] While calculating EELS, the corrected form of the dielectric function, suggested by Mermin,[24] will be used:

$$\epsilon(q,L,w)=\epsilon_0+\{(1+i\Gamma/w)[\epsilon'(q,L,w+i\Gamma)-\epsilon_0]\}/\{1+(i\Gamma/w)[\epsilon'(q,L,w+i\Gamma)-\epsilon_0]/[\epsilon'(q,L,0)-\epsilon_0]\}.\tag{3}$$

Such a correction does not lead to significant changes in the final result.

We take the single-layer (23,0) nanotube (a zigzag nanotube with $\theta=0°$ and $r=9$ Å) as a model system to study the basic features of inter-$\pi$-band excitations. The dielectric functions corresponding to the $L=0$ and 1 excitations are shown, respectively, in Figs. 1(a) and 1(b) at $\Gamma=0$ and $q=0.2$ Å$^{-1}$. The real part $\epsilon_1(q,L,w)$ is shown by the solid curve, and the imaginary part $\epsilon_2(q,L,w)$ by the dashed curve. They exhibit similar features, namely, many divergent structures below 10 eV, and a featureless spectrum above that. The inter-$\pi$-band matrix element of Eq. (2b) is very small for the high-frequency excitations, so that $\epsilon(w)$ becomes featureless there. The divergent structures arise mainly from the 1D band effect, which has a divergent joint density of states (JDOS). The integration of $dk_y$ in Eq. (2a) could be expanded as $D(J,w_{vc};q,L)dw_{vc}$, where $D=|[\partial w_{vc}(J,k_y;q,L)]/\partial k_y|^{-1}$ is the JDOS at different $q$'s and $L$'s. The JDOS is divergent at certain frequencies ($w_d$'s), e.g., at $w_d$'s corresponding to states $k_y=-q/2$ for the $L=0$ excitations of the ($m$,0) nanotube. Furthermore, their divergent forms (not shown) are similar to those of the DOS.[4,7] The dielectric functions thus exhibit rich divergent structures there.

The band dispersions have other important consequences as to the form of $\epsilon_1$ and $\epsilon_2$. The conduction subbands are found to concave upwards at the band edge ($k_y=0$) for $E^c<\gamma_0$, and downwards for $E^c>\gamma_0$ [see Fig. 1(b) in Ref. 7];

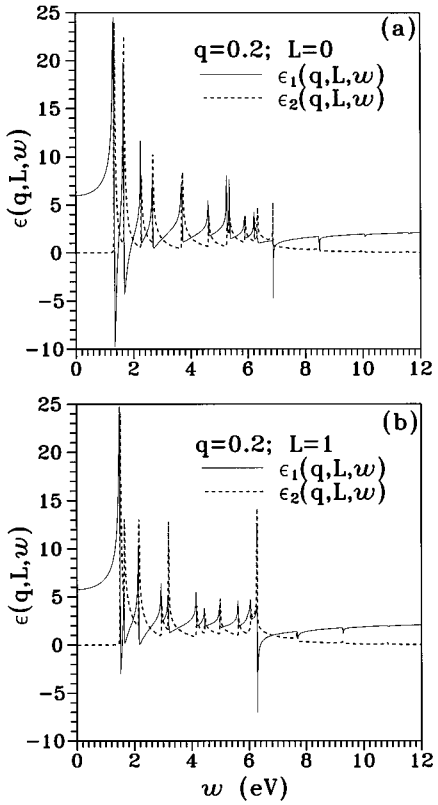


FIG. 1. The dielectric function of the (23,0) nanotube. $\epsilon_1(q,L,w)$ (solid curve) and $\epsilon_2(q,L,w)$ (dashed curve) are calculated at $\Gamma=0$, $q=0.2$ Å$^{-1}$, and (a) $L=0$ and (b) $L=1$. The unit of $q$ is Å$^{-1}$, here and henceforth.

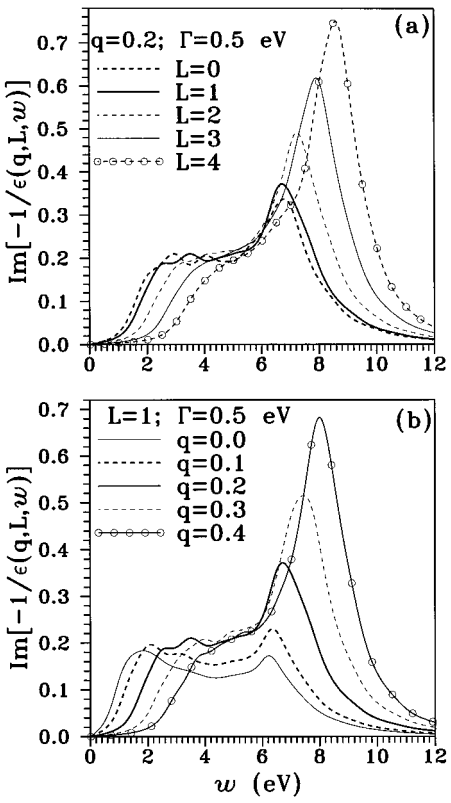


FIG. 2. The EELS of the (23,0) nanotube are calculated at $\Gamma=0.5$ eV, (a) $q=0.2$ Å$^{-1}$ and different $L$'s, and (b) $L=1$ and different $q$'s.

the valence subbands are symmetric to them about $E_F=0$. It is for these basic features that, in general, $\epsilon_1$ becomes negative and divergent only at $w>2\gamma_0$, which involves excitations related to those concave-downward conduction subbands above $\gamma_0$. Since plasmons are found where $\epsilon_1=0$ and $\epsilon_2$ is small, negative and divergent structures in $\epsilon_1$ at above $2\gamma_0$ cause plasmons at, and only at, $w>2\gamma_0$. These $\pi$ plasmons are found to cause a pronounced peak in EELS.[7] Zeros in $\epsilon_1$ at small $w$'s are associated with large $\epsilon_2$. They merely modify the $e$-$h$ excitations.

The EELS, defined as $\mathrm{Im}[-1/\epsilon(q,L,w)]$, is calculated at $\Gamma=0.5$ eV for a closer study of the $\pi$ plasmon. The results for five different $L$'s at $q=0.2$ Å$^{-1}$ are shown in Fig. 2(a). A pronounced peak, identified as the $\pi$ plasmon, exists in each of the spectra. The $\pi$ plasmon frequency ($w_p$) clearly increases as $L$ grows, maybe with the exception of the $L=0$ and 1 modes which are close to each other. The $L$-dependent plasmon excitations also depend on $q$. The $L=1$ spectra at different $q$'s are shown in Fig. 2(b). Again, $w_p$ increases with $q$, similar to the case shown in Fig. 2(a). This result confirms the early finding[12] that $q$ and $L$ play similar roles in a smaller nanotube.[12] All $L$-dependent plasmons also exhibit such a strong $q$ dependence.[23] In short, a carbon nanotube has a set of $L$-dependent plasmon modes, and each exhibits a strong $q$ dependence.

We have also studied the dependence of the $\pi$ plasmon on the nanotube geometry, such as its radius and chiral angle. The $\pi$ plasmon frequency is lower at smaller $q$'s and $L$'s. As shown in Fig. 2, $w_p$ is ~6–8 eV at $q<0.3$ Å$^{-1}$, and $L\leqslant 2$ for the (23,0) nanotube.[23] The ~6–8-eV plasmons are also found in other nanotubes. Figure 3 exemplifies the EELS from nanotubes of a wide range of chiral angles and radii. Some of these nanotubes are metallic and some are semiconducting, but they exhibit nearly the same plasmon frequencies at $q=0.2$ Å$^{-1}$ and $L=1$. The insensitivity of the plasmon structure to the nanotube geometry is mainly due to the characteristics of the $\pi$-band structure. Essentially, the con-

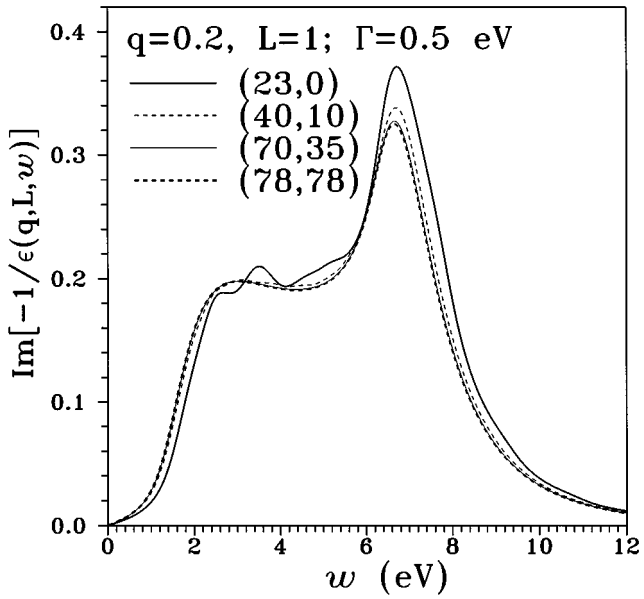


FIG. 3. The EELS of four carbon nanotubes: (23,0), (40,10), (70,35), and (78,78). They are calculated at $q=0.2$ Å$^{-1}$, $L=1$, and $\Gamma=0.5$ eV.

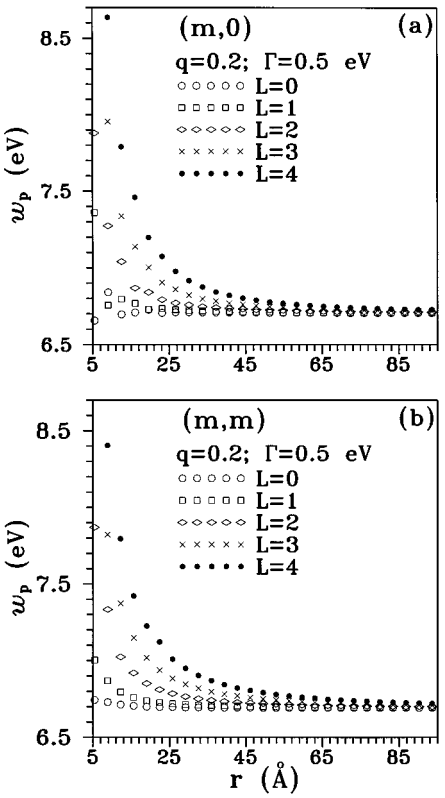


FIG. 4. The relation between radii ($r$'s) and $\pi$ plasmon frequencies ($m_p$'s) of different $L$'s, calculated at $q=0.2$ Å$^{-1}$ and $\Gamma=0.5$ eV for (a) zigzag nanotubes, and (b) armchair nanotubes.

duction bands are concave-downward only for those with $E^c(k_y=0)>\gamma_0$. Such a structure is a consequence of the $\pi$ band of a graphite sheet, and is only marginally modified due to the nanotube geometry.[7]

For a small nanotube as the one shown in Fig. 2(a), plasmon modes of different $L$'s are easily discernible in the EELS. However, the $L$ dependence in EELS becomes increasingly insignificant as the radius becomes larger; i.e., it crosses over from being a 1D nanotube to a 2D graphite sheet. Figures 4(a) and 4(b), respectively, show the plasmon frequency for the zigzag and armchair nanotube at $q=0.2$ Å$^{-1}$ as functions of the radius. Clearly $w_p$'s of different $L$'s merge together at large $r$. Roughly speaking, the $r$-dependence becomes insignificant at $r \gtrsim L/q$; the dimensionality crossover also depends on the momentum transfer.

Our results provide a reasonable explanation for the measured EELS. The EELS (Refs. 8–11) from a multilayer carbon nanotube shows that the $\pi$ plasmon frequency is ~5–7 eV. If the intertube interactions are neglected due to the large separation between the tubes, the total EELS is only the superposition of the spectra from several independent nanotubes. Then the measured plasmon structure agrees with our predicted 6–8-eV plasmon modes which exist for all carbon nanotubes at small $q$ and $L$. Intertube coupling could enhance the plasmon frequency somewhat,[23] but is unlikely to alter the conclusion reached above. It should be noticed that the predicted plasmon frequency is a function of the resonance integral (here $\gamma_0=3.033$ eV is used),[4] since plasmons lie at $w>2\gamma_0$ as explained earlier. Some estimations[2] put $\gamma_0$~2.4–2.7 eV. Smaller $\gamma_0$'s could then bring down the plasmon frequency to the measured value at ~5–7 eV.[23] The value of $\gamma_0$ can be independently determined from band measurement, e.g., using photoemission. The effects concerning the intertube coupling, the resonance integral $\gamma_0$, and the magnetic field, will be discussed elsewhere.

In conclusion, for carbon nanotubes we have calculated the longitudinal dielectric function, which is the $L$ dependent. The predicted 6–8-eV $\pi$ plasmons and their behavior, e.g., the crossover to 2D plasmons at large radius, could be experimentally checked with EELS or other optical spectra. The existence of a prominent 6–8-eV plasmon structure is the result of the unique $\pi$-band structure, and is supported by the ~5–7-eV plasmons observed in EELS.[8–11] The predicted strong $L$ and $q$ dependence have yet to be identified experimentally. The coupling effects in a multilayer nanotube, and a better determination of $\gamma_0$, are needed for a closer study of the problem.

This work was supported in part by the National Science Council of Taiwan, Republic of China under Grant Nos. NSC 85-2112-M-009-020 and NSC 85-2112-M-007-027.

[1] S. Iijima, Nature **354**, 56 (1991); S. Iijima and T. Ichihashi, *ibid.* **363**, 603 (1993).
[2] J. W. Mintwire *et al.*, Phys. Rev. Lett. **68**, 631 (1992); Phys. Rev. B **47**, 5485 (1993).
[3] N. Hamada *et al.*, Phys. Rev. Lett. **68**, 1579 (1992).
[4] R. Saito *et al.*, Appl. Phys. Lett. **60**, 2204 (1992); Phys. Rev. B **46**, 1804 (1992).
[5] X. Blase *et al.*, Phys. Rev. Lett. **70**, 1878 (1994).
[6] J. P. Lu, Phys. Rev. Lett. **74**, 1123 (1995); H. Ajiki and T. Ando, J. Phys. Soc. Jpn. **62**, 1255 (1993).
[7] M. F. Lin and K. W.-K. Shung, Phys. Rev. B **50**, 17 744 (1994).
[8] R. Kuzuo *et al.*, Jpn. J. Appl. Phys. **31**, L1484 (1992).
[9] P. M. Ajayan *et al.*, Phys. Rev. B **47**, 6859 (1993).
[10] L. A. Bursill *et al.*, Phys. Rev. B **49**, 2882 (1994).
[11] V. P. Dravid *et al.*, Science **259**, 1601 (1993).
[12] M. F. Lin and K. W.-K. Shung, Phys. Rev. B **47**, 6617 (1993); **48**, 5567 (1993).
[13] O. Sato *et al.*, Phys. Rev. B **48**, 1947 (1983).
[14] P. J. Lin-Chung and A. K. Rajagopal, Phys. Rev. B **49**, 8454 (1994).
[15] P. Longe and S. M. Bose, Phys. Rev. B **48**, 18 239 (1993).
[16] C. Yannouleas *et al.*, Phys. Rev. B **50**, 7977 (1994).
[17] P. S. Davids *et al.*, Phys. Rev. B **51**, 4557 (1995).
[18] H. Ehrenreich and M. H. Cohen, Phys. Rev. **115**, 786 (1959).
[19] E. A. Taft and H. R. Philipp, Phys. Rev. **138**, A197 (1965).
[20] P. R. Wallace, Phys. Rev. **71**, 622 (1947).
[21] M. F. Lin and K. W.-K. Shung, Phys. Rev. B **52**, 8423 (1995).
[22] K. W.-K. Shung, Phys. Rev. B **34**, 979 (1986).
[23] M. F. Lin and D. S. Chuu (unpublished).
[24] N. D. Mermin, Phys. Rev. B **1**, 2362 (1970).